PCCP

PAPER

Cite this: *Phys. Chem. Chem. Phys.*, 2016, **18**, 15645

Electrochemical and photophysical behavior of 1-naphthol in benzyl-*n*-hexadecyldimethylammonium 1,4-bis(2-ethylhexyl)sulfosuccinate large unilamellar vesicles

Airam K. Cobo Solis, N. Mariano Correa* and Patricia G. Molina*

Received 24th March 2016,
Accepted 11th May 2016

DOI: 10.1039/c6cp01979j

www.rsc.org/pccp

In the present contribution, 1-naphthol is investigated in large unilamellar vesicles formed from a new catanionic surfactant, benzyl-*n*-hexadecyldimethylammonium 1,4-bis(2-ethylhexyl)sulfosuccinate, by electrochemical and spectroscopic techniques. The electrochemical results show that 1-naphthol experiences a partition process between the water phase and the large unilamellar vesicle bilayer phase, which is corroborated by absorption spectroscopic studies at pH = 6.40 and pH = 10.75. Interestingly, studies of 1-naphthol emission in benzyl-*n*-hexadecyldimethylammonium 1,4-bis(2-ethylhexyl)sulfosuccinate large unilamellar vesicles at pH = 10.75 and in sodium 1,4-bis(2-ethylhexyl)sulfosuccinate water solution show that when the 1,4-bis(2-ethylhexyl)sulfosuccinate moiety is part of the bilayer, the 1,4-bis(2-ethylhexyl)sulfosuccinate polar head interacts strongly with 1-naphthol, by favoring emission from the excited neutral species resulting in the appearance of a new band close to λ = 355 nm. It seems that the large unilamellar vesicle bilayer of the catanionic vesicle slows down the proton transfer process observed in water, where only emission from 1-naphtholate is detected.

Introduction

Vesicles and liposomes are spherical aggregates formed by some amphiphilic compounds, in which the lipid bilayer surrounds an aqueous void volume that can be "loaded" with almost any variety of water-soluble marker molecules.[1,2] In general, large unilamellar vesicles (LUVs) are prepared for the application of different techniques (such as ultrasonication or extrusion) which involve a long and laborious preparation method. Nowadays, practical procedures to convert multilamellar vesicles (formed spontaneously) into LUVs are required.[3–5]

In our laboratory, a new catanionic surfactant, benzyl-*n*-hexadecyldimethylammonium 1,4-bis(2-ethylhexyl)sulfosuccinate (AOT–BHD), was synthesized from two traditional ionic surfactants (the anionic sodium 1,4-bis-2-ethylhexylsulfosuccinate (AOT) and the cationic benzyl-*n*-hexadecyldimethylammonium chloride (BHDC)). This "true" catanionic surfactant emerges when ionic surfactants are mixed in a 1 : 1 ratio, and the inorganic salt is totally removed. The formation of the catanionic surfactant was confirmed by the ^{1}H NMR technique in a previous work.[6] In general, when a cationic surfactant solution and an anionic surfactant solution are mixed, the reduction in area per headgroup resulting from ion pairing induces the formation of molecular bilayers and vesicles may be established spontaneously.[7–10] However, the formation of vesicles without salt is still an important challenge. The spontaneous formation and shape of the AOT–BHD vesicles were characterized by using dynamic light scattering (DLS) and small-angle X-ray scattering (SAXS) techniques.[6]

Although these systems show very different properties compared to the original surfactants,[11,12] studies on the properties of the self-assembled aggregates in aqueous solutions formed by this kind of true catanionic surfactants are scarce.[6] Very recently it has been shown that the bilayer of the AOT–BHD LUVs is very different from the typical one formed with traditional phospholipid 1,2-di-oleoyl-*sn*-*glycero*-3-phosphatidylcholine, DOPC. We found that the part of the bilayer close to the polar head of AOT–BHD is a powerful electron donor environment. Moreover, the AOT–BHD bilayer offers a less polar and slightly more viscous zone than DOPC.[13] On the other hand, what has not been investigated yet is the effect that the bilayer has on the proton transfer process, which is important because these processes are the most common in biological systems and have a significant role in obtaining mechanistic insights into biochemical reactions.[14]

The interactions of small molecules with membranes are important issues in membrane biology. Understanding their role in modulating the structure and function of biological membranes requires the knowledge of the location of the molecules.[15–17]

Electrochemical methods, such as cyclic voltammetry (CV) and square wave voltammetry (SWV), have been used to determine

Departamento de Química, Facultad de Ciencias Exactas, Físico-Químicas y Naturales, Universidad Nacional de Río Cuarto, Agencia Postal No 3 – (5800), Río Cuarto, Argentina. E-mail: acobosolis@exa.unrc.edu.ar, mcorrea@exa.unrc.edu.ar, pmolina@exa.unrc.edu.ar; Fax: +54 358 467 6233; Tel: +54 358 467 6111

partition coefficients for different drugs.[4,18,19] Regarding these techniques, there have been efforts on using these systems for the generation and amplification of electrochemical signals.[20–26] It is noteworthy that electrochemical techniques have an advantage over spectroscopic techniques since they may be used to eliminate the scattering due to the size of the aggregates. The scattering of the solution makes it almost unfeasible to investigate concentrated vesicle solutions (due to their turbidity) that are necessary for molecules whose partition constant values are low.

We have studied the behavior of 1-naphthol (NPh) in water and in LUVs formed from the phospholipid DOPC by SWV and CV techniques. These studies were compared with emission spectroscopic data. In DOPC LUV media, the redox behavior of NPh shows that the molecule undergoes a partition process between two phases, the water phase and the LUV bilayer phase. The electrochemical responses NPh allow us to propose a model to explain the electrochemical experimental results and, in conjunction with our measurements, to calculate the partition constant (K_p) value of NPh between the phases.[3] A molecular probe is chosen because its role is very important in industry.[27] In addition, NPh isomers are known for their hazardous effects on the environment and human health.[28] NPh is a nonionic, optical, hydrophilic and electroactive molecule which can help us to investigate in this work if the electrochemical and spectroscopy studies are viable to quantify its partitioning process between water and the AOT–BHD bilayer, and to understand the behavior of the interface of these new vesicles with regard to the proton transfer process.

Since this new system can be used as a drug delivery agent, which is a field that we are currently investigating, it is very important to characterize the physicochemical properties of the bilayer. In the present contribution, we want to expand the study of this interesting probe by investigating its electrochemical and photophysical behavior in AOT–BHD LUVs. The electrochemical results confirm that NPh experiences a partition process between the water phase and the LUV bilayer phase, which is corroborated by absorption spectroscopic research. Studies of NPh emission in AOT–BHD LUVs at pH = 10.75 in NaAOT water solution show that when the AOT moiety is part of the bilayer, the AOT polar head interacts strongly with NPh favoring the emission from the excited neutral species, NPh*, resulting in the appearance of a new band close to λ = 355 nm. It seems that the LUV catanionic bilayer slows down the proton transfer process observed in water, where only emission from 1-naphtholate (NPh^-) species is detected.

Experimental section

Materials

Sodium 1,4-bis(2-ethylhexyl)sulfosuccinate (NaAOT), from Sigma (>99% purity), was used as received. Benzyl-*n*-hexadecyldimethylammonium chloride (BHDC), from Sigma (>99% purity), was recrystallized twice from ethyl acetate.[29–31] NPh, from Sigma-Aldrich, was used without further purification.

Methods

The catanionic surfactant used AOT–BHD was obtained by means of a method reported in ref. 6. In a round-bottom flask, equimolar fractions of NaAOT/dichloromethane and BHDC/dichloromethane solutions were combined and stirred at room temperature for 72 hours. During stirring, a white precipitate was formed, which was attributed to NaCl formation from the original surfactant counterions. The majority of NaCl was discarded from the dichloromethane solution by centrifugation. Thereafter the dichloromethane solution containing AOT–BHD was washed with small amounts of water until the aqueous fraction was observed to be free of chloride ($AgNO_3$ test). After the NaCl was eliminated, the dichloromethane was removed by vacuum evaporation. After isolating AOT–BHD, it was purified by mixing with activated charcoal, then filtered through a plug of neutral alumina into a round-bottom flask, dried under vacuum and stored under nitrogen. The new surfactant obtained, AOT–BHD, was a colorless highly viscous liquid with a melting point below 100 °C and very low vapor pressure. These characteristics are dramatically distinct from NaAOT and BHDC since both surfactants have high melting points.

After the solvent was evaporated and the film was dried under reduced pressure, LUVs were obtained by hydrating using 0.70×10^{-4} M, 1.00×10^{-4} M, and 2.00×10^{-3} M NPh for spectroscopic and electrochemical measurements respectively, and 0.05 M $LiClO_4$.

Measurements

The absorption spectra were measured by using Shimadzu 2401 equipment at 25.0 ± 0.1 °C using cell diffuse spectroscopy (integrating sphere) which allows elimination of the effect of light scattering caused by the high turbidity solutions. A Spex fluoromax apparatus was employed for the fluorescence measurements. Corrected fluorescence spectra were obtained using the correction file provided by the manufacturer. The path length used in the absorption and emission experiments was 1 cm. The uncertainties in λ_{max} were about 0.1 nm. To subtract the background contribution of the absorption and emission spectra, samples of the same concentrations of vesicles were prepared by omitting the addition of the probes.

The diameters and the diffusion coefficient of LUVs were determined by dynamic light scattering (DLS, Malvern 4700 with goniometer and 7132 correlator) with an argon-ion laser operating at 488 nm at two different pH values. The apparent diameter and the diffusion coefficient values obtained are 82 ± 5 nm and $2.2 \pm 0.3 \times 10^{-7}$ cm^2 s^{-1} (pH = 10.75), and 78 ± 5 nm and $2.3 \pm 0.2 \times 10^{-7}$ cm^2 s^{-1} (pH = 6.4) independent of the AOT–BHD concentration investigated, which shows that the vesicle–vesicle interactions are weak.[6] All the measurements were carried out at a scattering angle of 90° at a temperature of 25.0 ± 0.1 °C. The measurements were made by diluting the samples in a cuvette with distilled water. The water was filtered three times by using an Acrodisc with a 0.45 μm Nylon membrane (Agilen) to avoid dust or particles before use. Since we have worked with diluted solutions, the refractive indices

and viscosities for the vesicle solutions were assumed to be the same as the external solvent.[32] Multiple samples at each size were made, and thirty independent size measurements were made for each individual sample at a scattering angle of 90°. The instrument was calibrated before and during the course of experiments by using several different size standards. Thus, we are confident that the magnitudes obtained by DLS measurements can be statistically significant for all the systems investigated. The DLS experiments show that the polydispersity of the LUV size is less than 5%.

An AutoLab PGSTAT 30 potentiostat, controlled by the GPES 4.8 software, was employed for SWV measurements. The characteristic parameters used to obtain square wave voltammograms are as follows: 0.025 V for the square wave amplitude (ΔE_{SW}), 0.005 V for the staircase step height (ΔE_s) and 20 Hz for the frequency (f). The working electrode was a Pt disk (area = 0.126 cm^2). It was polished, sonicated, and copiously rinsed with distilled water. For the purpose of obtaining good response the electrode was cycled several times in the blank solutions (0.05 M $LiClO_4$) prior to use until reproducible responses in current were obtained. The counter electrode was a Pt foil of large area (2 cm^2). A freshly prepared Ag/AgCl quasi-reference electrode was used. All the experiments were performed under a purified nitrogen atmosphere at 25.0 ± 0.1 °C. The pH measurements were performed by using an Orion 720A pH meter that was calibrated with commercial buffers. pH values of 6.40 and 10.75 were obtained for different solutions; a solution of 6.00 M Na(OH) was used for adjusting the pH to 10.75, at which the NPh is dissociated since the pK_a of NPh is 9.34.[33]

OriginPro 8.0 was used for analysis and calculations.

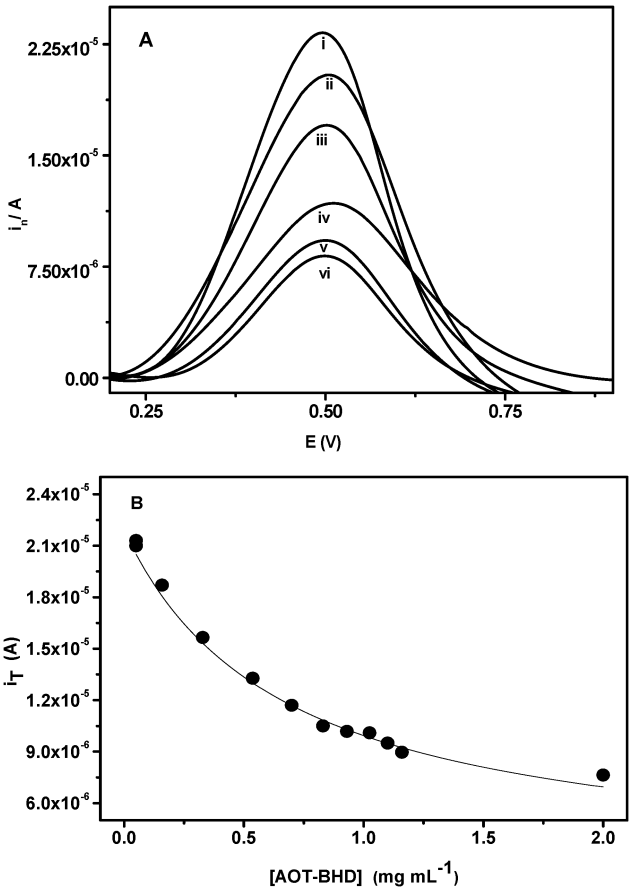

Fig. 1 (A) Square wave voltammograms of NPh for different AOT–BHD concentrations: (i) 0.00, (ii) 0.07, (iii) 0.30, (iv) 0.80, (v) 1.10 and (vi) 2.00 mg mL^{-1}. [NPh] = 2.00 × 10^{-3} M, ΔE_s = 5 mV, ΔE_{SW} = 25 mV, f = 20 Hz in [$LiClO_4$] = 0.05 M, pH = 6.40. (B) Dependence of the net total current on the AOT–BHD concentration; [NPh] = 2.00 × 10^{-3} M in [$LiClO_4$] = 0.05 M. Experimental data (●) and the solid line (—) is the fitting of the experimental data to eqn (7).

Results and discussion

Electrochemical studies

In Fig. 1A, the net current peak (i_n) of SW voltammograms corresponding to NPh in water and NPh in AOT–BHD LUVs of different concentrations at pH = 6.40 respectively is shown. Although the profile in Fig. 1A–i in water is analogous to that obtained in vesicles (Fig. 1A–ii–vi), a difference can be immediately observed: despite the fact that NPh concentration is constant, the i_n values are lower than those in water, and decrease with the AOT–BHD concentration.

The decrease in i_n values with the AOT–BHD concentration could be due to the fact that NPh undergoes a partition process in both phases, water and the LUV bilayer, according to eqn (1):

$$[\mathrm{NPh}]_W + [\mathrm{AOT\text{–}BHD}] \rightleftarrows [\mathrm{NPh}]_{LUVs} \quad (1)$$

The i_n values change because the diffusion coefficient of the electroactive species incorporated within the LUV bilayer is smaller than that in water. Therefore, the electroactive species are NPh in the water pseudophase ($[\mathrm{NPh}]_W$) and NPh incorporated into the LUV bilayer pseudophase ($[\mathrm{NPh}]_{LUVs}$).

In LUV media, the NPh partition process between AOT–BHD LUVs and water pseudophases is treated within the framework of the pseudophase model.[34] Thus, the distribution of NPh between the bilayer and the water phase defined in eqn (1) is expressed in terms of the partition constant K_p shown in eqn (2):

$$K_p = \frac{[\mathrm{NPh}]_{LUVs}}{[\mathrm{NPh}]_W[\mathrm{AOT} - \mathrm{BHD}]} \quad (2)$$

In Fig. 1A, there is only one voltammetric peak confirming that NPh present in both phases is oxidized simultaneously at the same potential.

The total peak current, i_T, has two contributions as shown in eqn (3):

$$i_T = a[\mathrm{NPh}]_W + b[\mathrm{NPh}]_{LUVs} \quad (3)$$

where

$$a = nFA\left(\frac{D_W}{\pi t_p}\right)^{\frac{1}{2}}\phi \quad (4)$$

and

$$b = nFA\left(\frac{D_{\mathrm{LUVs}}}{\pi t_{\mathrm{p}}}\right)^{\frac{1}{2}}\phi \quad (5)$$

where n is the electron number transferred per molecule, A is the electrode area, F is the Faraday constant, D_{W} and D_{LUVs} are the NPh diffusion coefficients in water and the vesicle respectively, ϕ is the current function of SWV and t_{p} is the pulse time of SWV and $t_{\mathrm{p}} = 1/2f$ where f is the frequency of SWV.[3]

The total concentration of NPh is expressed in eqn (6):

$$[\mathrm{NPh}]_{\mathrm{T}} = [\mathrm{NPh}]_{\mathrm{W}} + [\mathrm{NPh}]_{\mathrm{LUVs}} \quad (6)$$

By substituting eqn (3) and (4) in eqn (2), we obtain eqn (7):

$$i_{\mathrm{T}} = [\mathrm{NPh}]_{\mathrm{T}}\left[\frac{a + bK_{\mathrm{p}}[\mathrm{AOT-BHD}]}{1 + K_{\mathrm{p}}[\mathrm{AOT-BHD}]}\right] \quad (7)$$

The experimental data shown in Fig. 1B were fitted to eqn (7) by using a nonlinear regression method to determine D_{LUVs} and K_{p} values simultaneously.[3] In order to obtain the value of D_{LUVs}, a and b parameters should be replaced in eqn (4) and (5) where a value of $D_{\mathrm{W}} = 2.17 \times 10^{-5}$ cm^2 s^{-1} and $n = 1$ are used from ref. 3. This assumption is based on the fact that the NPh discharge in water and vesicles agrees with that observed previously in ref. 3. Fitting values calculated from eqn (7) at pH = 6.40 were $a = 10.97 \pm 0.05$, $b = 1.07 \pm 0.04$ and $R^2 = 0.99$.

The same procedure was carried out at pH = 10.75, but now the ionized species NPh^- is the one distributed between the two phases. The results are shown in Fig. 2A and B respectively. Fitting values calculated from eqn (7) at pH = 10.75 were $a = 29.02 \pm 0.02$, $b = 2.84 \pm 0.02$, and $R^2 = 0.99$.

The K_{p} and D_{LUVs} values are gathered in Table 1, where experimental values obtained by using DLS, an independent technique, are also included for comparison at pH = 6.40 and pH = 10.75. As can be seen, the D_{LUVs} values obtained from electrochemical measurements are within the experimental error, similar to those obtained by using DLS under the same conditions. Besides, from these D_{LUVs} values, it can be seen that comparable vesicle sizes are obtained with reports shown earlier.[6] The lower K_{p} value for NPh^- suggests that neutral species, NPh, has higher affinity for the bilayer which is reasonable as the ionized species has a negative charge that can be repelled by the polar heads of the surfactants.

Absorption spectroscopy studies

We also have used other independent technique, absorption spectroscopy, in order to obtain the K_{p} value to compare with the value obtained through the electrochemical procedure.

The values of K_{p} can be determined from the changes with the AOT–BHD concentration in the NPh absorption spectra at pH = 6.40 and pH = 10.75.[35–37]

Thus, for NPh K_{p} was determined by using eqn (8):[37,38]

$$A^{\lambda} = \frac{(\varepsilon^{\mathrm{f}} + \varepsilon^{\mathrm{b}}[\mathrm{AOT-BHD}]K_{\mathrm{p}})[\mathrm{NPh}]_{\mathrm{T}}}{1 + K_{\mathrm{p}}[\mathrm{AOT-BHD}]} \quad (8)$$

where A^{λ} is the absorbance at different surfactant concentrations, ε^{f} and ε^{b} are the molar extinction coefficients for NPh in water and AOT–BHD vesicles respectively, and $[\mathrm{NPh}]_{\mathrm{T}}$ is the total NPh concentration. It should be noted that ε^{f} was determined experimentally from the spectra of NPh in water at $\lambda = 290$ nm ($\varepsilon^{\mathrm{f}} = 4233.2 \pm 0.1$ mol^{-1} L cm^{-1}) for pH = 6.40 and $\lambda = 335$ nm ($\varepsilon^{\mathrm{f}} = 6350.9 \pm 0.1$ mol^{-1} L cm^{-1}) for pH = 10.75. The ε^{b} was obtained from the fitting of the experimental data by using eqn (8) for both pH values.

Fig. 3A and B show typical absorption spectra varying the AOT–BHD concentration at pH = 6.40 and pH = 10.75, respectively.

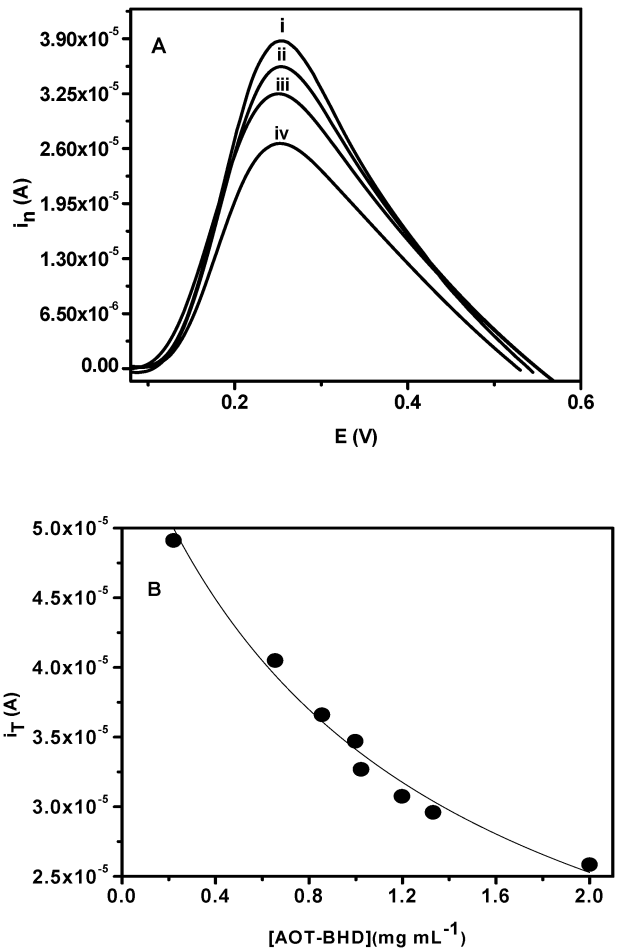

Fig. 2 (A) Square wave voltammograms of NPh for different AOT–BHD concentrations: (i) 0.60, (ii) 0.80, (iii) 1.00 and (iv) 2.00 mg mL^{-1}. [NPh^-] = 2.00×10^{-3} M, $\Delta E_{\mathrm{s}} = 5$ mV, $\Delta E_{\mathrm{SW}} = 25$ mV, $f = 20$ Hz in [$LiClO_4$] = 0.05 M, pH = 10.75 was adjustment with a 6.00 M Na(OH) solution. (B) Dependence of the net total current on the AOT–BHD concentration; [NPh^-] = 2.00×10^{-3} M in [$LiClO_4$] = 0.05 M, pH = 10.75. Experimental data (●) and the solid line (—) is the fitting of the experimental data to eqn (7).

Table 1 NPh partition constant, K_{p}, and the diffusion coefficient of AOT–BHD vesicles, D_{LUVs}, obtained by using different techniques

pH	Technique	K_{p} (mL mg^{-1})	D_{LUVs} (cm^2 s^{-1})
6.4	SWV	1.55 ± 0.03	$(2.06 \pm 0.03) \times 10^{-7}$
6.4	Absorption spectroscopy	1.2 ± 0.2	
10.75	SWV	0.84 ± 0.01	$(2.08 \pm 0.03) \times 10^{-7}$
10.75	Absorption spectroscopy	0.7 ± 0.1	
6.4	DLS		$(2.3 \pm 0.3) \times 10^{-7}$
10.75	DLS		$(2.2 \pm 0.2) \times 10^{-7}$

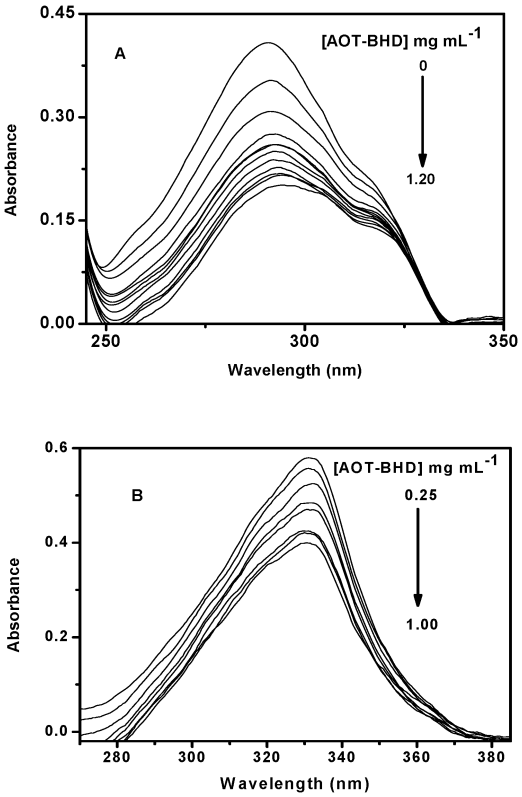

Fig. 3 Absorption spectra of NPh at pH = 6.40 (A) and NPh^- at pH = 10.75 (B) at different AOT–BHD concentrations. [NPh] = 1.00 × 10^{-4} M.

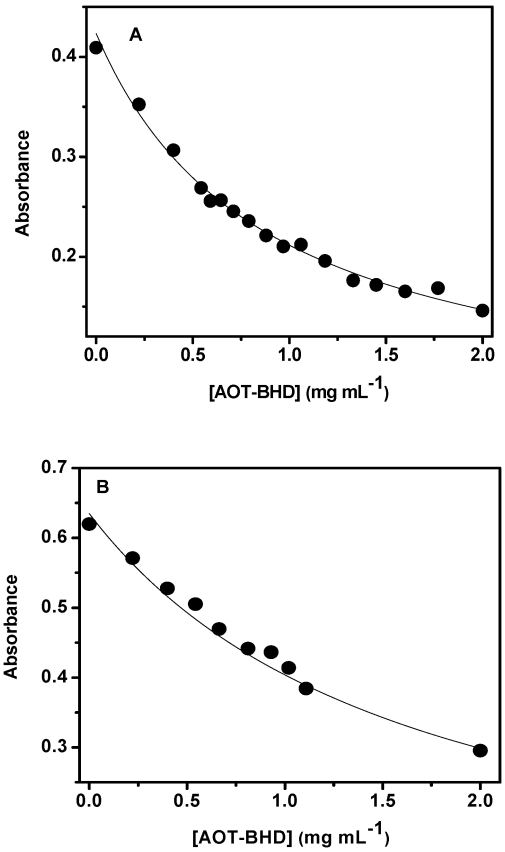

Fig. 4 Dependence of absorbance at λ = 290 nm with the AOT–BHD concentration at pH = 6.40 (A), and λ = 332 nm at pH = 10.75 (B). Experimental data (●) and the solid line (—) is the fitting of the experimental data to eqn (8). [NPh] = 1.00 × 10^{-4} M.

Fig. 3 clearly shows the decrease in the absorbance value with increasing AOT–BDH concentration, indicating the incorporation of the probe into the bilayer. The absorbance values obtained for different [AOT–BHD] are shown in Fig. 4A and B. These data were fitted to eqn (8) by using a nonlinear regression method, and the K_p values obtained for each pH are gathered in Table 1.

Also, it can be seen in Fig. 4 that, at [AOT–BHD] > 1.50 mg mL^{-1} the absorbance values do not change significantly which suggests that NPh and NPh^- are totally incorporated into the bilayer.

The K_p values obtained by using eqn (8) are comparable (within the experimental error of both techniques) to that obtained by means of SWV.

Emission spectroscopy studies

In order to obtain information about the effect that the bilayer has on the proton transfer process, we have used the emission spectroscopy of NPh embedded in the bilayer. In general, phenols become more acidic in the excited state and their pK_a decreases by several units in the electronically excited state (pK_a* around 0.5)[39] compared to that in the ground state (pK_a around 9).[39–41] As a consequence, if the pH of the medium is intermediate between the pK_a in the ground and the excited states, in the ground state the molecule stays in the neutral form at pH < 9, while in the excited state, it readily deprotonates to produce the anion (NPh^{*-}) in which state it emits. Thus, in aqueous solution (see Scheme 1 on the left), NPh undergoes ultrafast deprotonation in 35 ps, and the intensity of the neutral emission of NPh* (at 355 nm) is extremely low in aqueous solution and one observes almost exclusively the anion emission of NPh^{*-} at λ = 460 nm.[3]

On the other hand, the situation is quite different in a constrained environment such as the bilayer. For example, for NPh in the presence of DOPC vesicles it was observed that two emission bands were detected at λ = 355 nm and λ = 460 nm which were assigned to the neutral and anionic species, respectively. This feature was explained by considering that the excited state deprotonation of NPh is significantly retarded in a confined environment such as micelles and vesicles.[3] Thus, the NPh species also emits from the phenol located at the DOPC bilayer.[3] In other words, in aqueous media at pH = 6.40, NPh in the ground state exists exclusively as a neutral species but, after excitation, NPh rapidly dissociates into the anionic naphtholate (NPh^-) species and the emission comes exclusively from the anionic species (at λ = 460 nm). It is also important to note that in the case of DOPC LUVs[3] no equilibrium is established between the neutral form and the anion form, in the electronically excited state when NPh binds to the DOPC vesicles, and also, there is no diffusion of the excited species among the different phases. The failure to establish an equilibrium may be ascribed to the extreme slowness of the transfer back of the proton of the NPh^- species. In the DOPC vesicles,

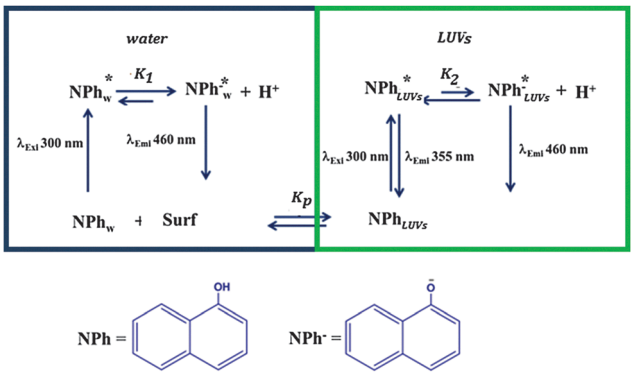

Scheme 1 Schematic representation of the different emission NPh species in the different pseudophases.

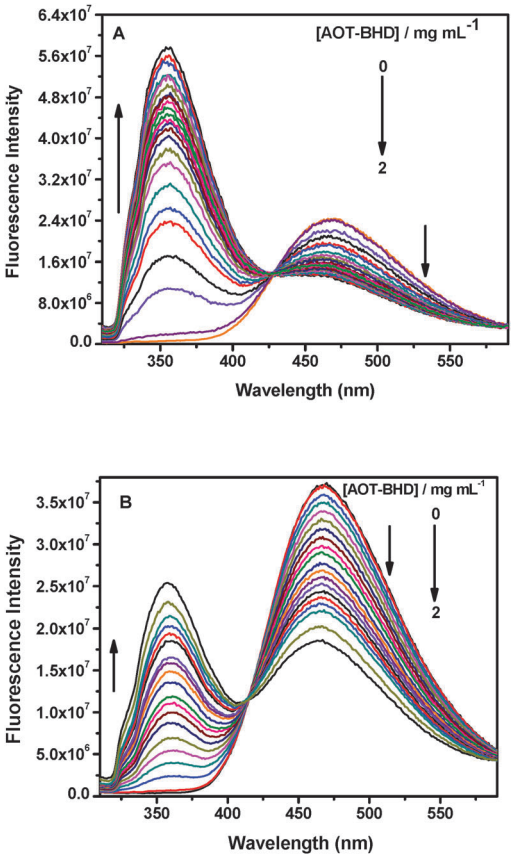

Fig. 5 (A) Emission spectra (λ_{exc} = 300 nm) of NPh at different AOT–BHD concentrations from 0.00 mg mL^{-1} to 2.00 mg mL^{-1}, [NPh] = 0.70 × 10^{-4} M in [$LiClO_4$] = 0.05 M, pH = 6.40. (B) Emission spectra (λ_{exc} = 300 nm) of NPh^- at different AOT–BHD concentrations from 0.00 mg mL^{-1} to 2.00 mg mL^{-1}, [NPh^-] = 1.00 × 10^{-4} M in [$LiClO_4$] = 0.05 M, pH = 10.75 was adjusted with a 6.00 M Na(OH) solution.

NPh undergoes the partition process between the two phases and, for the species that exists at the bilayer, deprotonation in the excited state is retarded and the emissions from both species are detected. This is probably due to the effect of the confinement and the low polarity that the bilayer has, in comparison with pure water. Fig. 5A shows the NPh emission spectra at different [AOT–BHD] at pH = 6.40. The data show the incorporation of the probe into the bilayer by the appearance of two bands as explained for DOPC vesicles. This figure shows that on increasing [AOT–BHD] the band that corresponds to the anionic species (λ = 460 nm) begins to decrease and the other one that belongs to the neutral species begins to increase (λ = 355 nm) with the presence of a neat isoemissive point at λ = 427 nm.

All these results suggest that, in contrast to what was previously observed in the DOPC bilayer,[3] in the AOT–BHD system, an equilibrium is established in the excited state. Moreover, it seems that it is shifted to the NPh* neutral species formation by the presence of the AOT–BHD LUVs (see Scheme 1 right part).

Fig. 5B shows the same study performed at pH = 10.75 where in the ground state only the anionic species (NPh^-) exists. In the absence of AOT–BHD a single band emission from the excited ionized species is observed. On the other hand, as [AOT–BHD] increases, a new band begins to appear at λ = 355 nm indicating the presence, in the excited state, of the NPh neutral species even at pH = 10.75. This result suggests that the bilayer favors the formation of the neutral species in the excited state despite the high pH value. A question may arise here because it is known that the sulfonate group of NaAOT in reverse micellar media is exceptional as a hydrogen bond acceptor.[42–44] So it is good that in AOT reverse micellar media with an HO^- concentration of around 0.1 M, neutral phenol species are the only ones present because of the strong hydrogen bond interaction with the AOT polar head.[42] Thus, is the AOT moiety of the AOT–BHD surfactant responsible for this unusual behavior? Furthermore, is the sulfonate group of the free AOT or the surfactant forming reverse micelles or being part of a bilayer for this unique behavior? In order to answer this question we performed experiments by using NaAOT dissolved in water forming direct micelles. Fig. 6 shows an emission spectrum of NPh at pH = 10.75 in a water solution containing [AOT] = 2.25 × 10^{-3} M, the same [AOT] present in AOT–BHD LUVs. As can be seen, only one band is detected at λ = 460 nm which corresponds to the emission of the excited species ionized. The conclusion that can be arrived at is that in the excited state under these conditions, only the ionized species is detected. Thus, it seems that AOT only shows the outstanding hydrogen bond acceptor capacity when it is part of the vesicle bilayer or reverse micelles. This behavior confirms once again that the properties of the original surfactant change when organized to form vesicles.[11,12]

Therefore, studies of emission for NPh at pH = 10.75 in AOT–BHD LUVs and AOT show that when the AOT is part of the bilayer, the AOT polar head interacts strongly, through hydrogen bonding, with NPh favoring the formation of the neutral NPh* species resulting in the appearance of the band close to λ = 355 nm. These results could have a tremendous impact on chemical reactions occurring in AOT–BHD vesicles, such as acid–base and/or enzyme-catalyzed reactions.

By following this idea and in order to determine the acid–base equilibrium constant of the excited NPh species at the bilayer, K_2, and $[NPh]_{LUVs}^{*-}$ (see Scheme 1 on the right) at pH = 6.40 and pH = 10.75 we propose the following model with the following assumption:

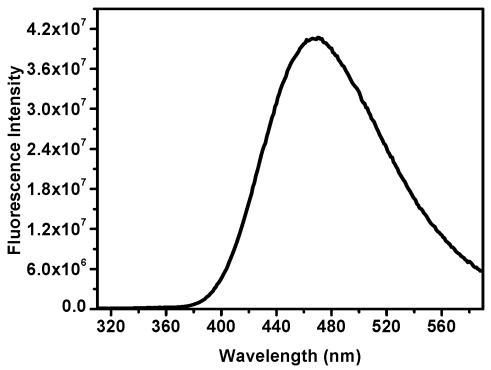

Fig. 6 Emission spectra (λ_{exc} = 300 nm) of NPh in a solution with a concentration of 2.25 × 10^{-3} M AOT, [NPh] = 1.00 × 10^{-4} M in [$LiClO_4$] = 0.05 M, pH = 10.75 was adjusted with a 6.00 M Na(OH) solution.

The K_2 value is small in comparison with the one in pure water (K_1 = 0.31)[39] since emission from the neutral species is detected in the bilayer (Fig. 5A).

$$[\mathrm{NPh}]_{\mathrm{LUVs}}{}^{*-} \ll [\mathrm{NPh}]_{\mathrm{LUVs}}{}^{*} \quad (9)$$

Since $[\mathrm{NPh}]_{\mathrm{LUVs}}{}^{*-}$ is negligible compared to $[\mathrm{NPh}]_{\mathrm{LUVs}}{}^{*}$, according to Scheme 1

$$[\mathrm{NPh}]_{\mathrm{LUVs}} \approx [\mathrm{NPh}]_{\mathrm{LUVs}}{}^{*} \quad (10)$$

The equilibrium of Scheme 1 (right part) can be expressed as

$$\mathrm{NPh}_{\mathrm{LUVs}}{}^{*} \rightleftarrows \mathrm{NPh}_{\mathrm{LUVs}}{}^{*-} + \mathrm{H}^{+} \quad (11)$$

Using eqn (10) and (11) K_2 is obtained:

$$K_2 = \frac{[\mathrm{NPh}]_{\mathrm{LUVs}}{}^{*-}[\mathrm{H}^{+}]}{[\mathrm{NPh}]_{\mathrm{LUVs}}{}^{*}} = \frac{x^2}{[\mathrm{NPh}]_{\mathrm{LUVs}}{}^{*} - x} \quad (12)$$

where x is $[\mathrm{NPh}_{\mathrm{LUVs}}{}^{*-}]$ and $[\mathrm{H}^{+}]$ present at equilibrium as shown in eqn (11).

According to eqn (9), x can be neglected in the denominator of eqn (12) and by combining eqn (2), (6) and (12) the following equation is obtained:

$$[\mathrm{NPh}]_{\mathrm{LUVs}}{}^{*} = K_{\mathrm{p}}\left([\mathrm{NPh}]_{\mathrm{T}} - \frac{x^2}{K_2}\right)[\mathrm{AOT-BHD}] \quad (13)$$

At λ_{Emi} = 355 nm eqn (14) can be expressed as[45]

$$I = 2.303 I_0 \phi \varepsilon [\mathrm{NPh}]_{\mathrm{LUVs}}{}^{*} \quad (14)$$

where I_0 is the intensity of incident light, and ϕ and ε are the quantum efficiency and molar absorptivity coefficients of $[\mathrm{NPh}]_{\mathrm{LUVs}}{}^{*}$ respectively.

By substituting $[\mathrm{NPh}]_{\mathrm{LUVs}}{}^{*}$ obtained from eqn (13) in eqn (14) the following equation is obtained:

$$I = 2.303 I_0 \phi \varepsilon K_{\mathrm{p}}\left([\mathrm{NPh}]_{\mathrm{T}} - \frac{x^2}{K_2}\right)[\mathrm{AOT-BHD}] \quad (15)$$

The emission intensity obtained for different [AOT–BHD] at λ_{Emi} = 355 nm (λ_{Exc} = 300 nm) is shown in Fig. 7A and B. These data were fitted to eqn (15) by using a nonlinear regression method and, the K_2 and $[\mathrm{NPh}]_{\mathrm{LUVs}}{}^{*-}$ values for pH = 6.40 and pH = 10.75 obtained for each pH are gathered in Table 2.

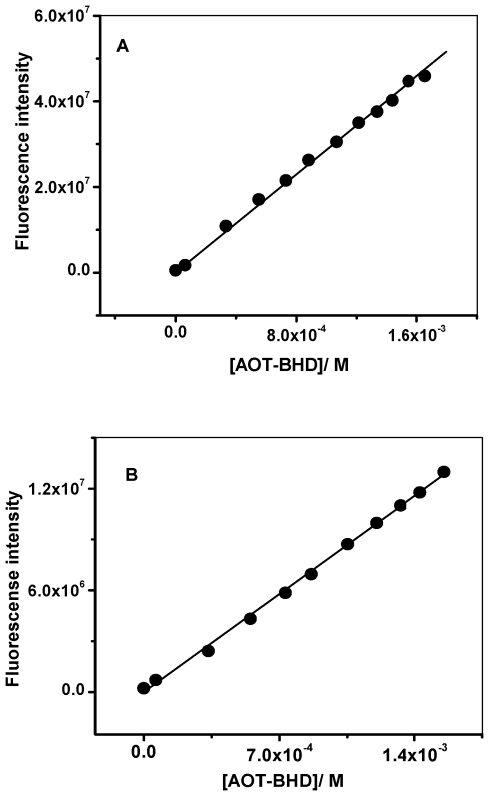

Fig. 7 (A) Dependence of the fluorescence intensity at λ_{Emi} = 355 (λ_{exc} = 300 nm) on the AOT–BHD concentration; [NPh^-] = 0.70 × 10^{-4} M, pH = 6.40. Experimental data (●) and the solid line (—) is the fitting of the experimental data to eqn (15). (B) Dependence of the fluorescence intensity at λ_{Emi} = 355 (λ_{exc} = 300 nm) on the AOT–BHD concentration; [NPh^-] = 1.00 × 10^{-4} M, pH = 10.75. Experimental data (●) and the solid line (—) is the fitting of the experimental data to eqn (15).

Table 2 K_2 and $[\mathrm{NPh}]^{*-}$ values obtained from fitting the experimental data to eqn (15) for fluorescence intensity at λ_{Emi} = 355 nm. λ_{Exc} = 300 nm

pH	K_2	$[\mathrm{NPh}]^{*-}$ (M)	R^2
6.40	$(4.03 \pm 0.10) \times 10^{-11}$	$(5.31 \pm 0.01) \times 10^{-8}$	0.998
10.75	$(7.85 \pm 0.01) \times 10^{-10}$	$(2.80 \pm 0.02) \times 10^{-7}$	0.999

As can be observed, the K_2 value decreases dramatically in the vesicle bilayer in comparison with the value obtained in pure water. It seems that, in the AOT–BHD bilayer, the favored species is the neutral species, even at a high pH value. The strong hydrogen bond interaction between NPh and the AOT moiety may be the cause of this behavior. Scheme 2 shows schematically the interpretation of this interaction.

Conclusions

We have investigated the electrochemical behavior of NPh in the new large unilamellar vesicle system formed from the AOT–BHD surfactant by using electrochemical and spectroscopic techniques. In AOT–BHD large unilamellar vesicle media, the NPh behavior shows that the molecule undergoes a partition process between two phases, water and the large unilamellar

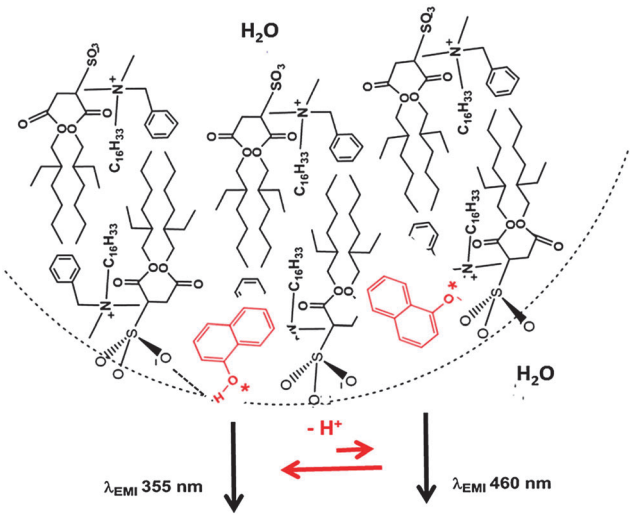

Scheme 2 Schematic representation of the hydrogen bond interaction between NPh and the vesicle bilayer.

vesicle bilayer. Also, by using an electrochemical model we could calculate the partition constant values at pH = 6.40 and pH = 10.75. The values of the partition constant show good agreement with the values obtained by absorbance spectroscopy under the same experimental conditions. Moreover, our model also allows us to calculate the diffusion coefficient in the vesicle for AOT–BHD large unilamellar vesicles, which coincides with the diffusion coefficient in the vesicle obtained through the dynamic light scattering technique. Thus, we confirm that the electrochemical technique is a powerful tool to characterize organized media such as large unilamellar vesicles as we have previously shown in ref. 3 in DOPC large unilamellar vesicles.

On the other hand, and in contrast to what was observed in other large unilamellar vesicle media formed from different phospholipids[3,39,40] and in micelles formed from different non-ionic, cationic and anionic surfactants,[41] we found that in the AOT–BHD large unilamellar vesicle bilayer, the acid equilibrium process of NPh is dramatically retarded and a clear isoemissive point is detected in its emission spectra, at different surfactant concentrations. Studies of NPh emission at pH = 10.75 and in NaAOT water solution show that when the AOT moiety is part of the bilayer, the polar head interacts strongly with NPh by favoring the emission from the excited neutral species of NPh with the consequent decreases in the equilibrium constant compared to the value in pure water. From these results the equilibrium constant in the exited state of NPh located in the bilayer was calculated for the first time.

We feel that our study could have an important impact on chemical reactions occurring in a bilayer, such as acid–base and/or enzyme-catalyzed reactions that we are currently investigating in this newly organized media.

Acknowledgements

Financial support from the Consejo Nacional de Investigaciones Científicas y Técnicas (CONICET), Universidad Nacional de Río Cuarto and Agencia Nacional de Promoción Científica y Técnica is gratefully acknowledged. AKCS, NMC and PGM hold a research position at CONICET. AKCS thanks CONICET for a research fellowship.

Notes and references

1 M. Kępczyński, K. Nawalani, B. Jachimska, M. Romek and M. Nowakowska, *Colloids Surf., B*, 2006, **49**, 22–30.
2 F. Moyano, M. A. Biasutti, J. J. Silber and N. M. Correa, *J. Phys. Chem. B*, 2006, **110**, 11838–11846.
3 J. S. Florez Tabares, M. L. Blas, L. E. Sereno, J. J. Silber, N. M. Correa and P. G. Molina, *Electrochim. Acta*, 2011, **56**, 10231–10237.
4 F. Moyano, P. G. Molina, J. J. Silber, L. E. Sereno and N. M. Correa, *ChemPhysChem*, 2010, **11**, 236–244.
5 R. R. C. New, *Liposomes: A practical approach*, Oxford University Press, New York, 1997.
6 C. C. Villa, F. Moyano, M. Ceolin, J. J. Silber, R. D. Falcone and N. M. Correa, *Chem. – Eur. J.*, 2012, **18**, 15598–15601.
7 J. Hao and H. Hoffmann, *Curr. Opin. Colloid Interface Sci.*, 2004, **9**, 279–293.
8 S. A. Safran, P. Pincus and D. Andelman, *Science*, 1990, **248**, 354–356.
9 E. W. Kaler, K. L. Herrington, A. Murthy and J. A. N. Zasadzinski, *J. Phys. Chem.*, 1992, **96**, 6698–6707.
10 M. P. Nieh, T. A. Harroun, V. A. Raghunathan, C. J. Glinka and J. Katsaras, *Biophys. J.*, 2004, **86**, 2615–2629.
11 B. F. B. Silva, E. F. Marques, U. Olsson and R. Pons, *Langmuir*, 2010, **26**, 3058–3066.
12 C. Banerjee, S. Mandal, S. Ghosh, J. Kuchlyan, N. Kundu and N. Sarkar, *J. Phys. Chem. B*, 2013, **117**, 3221–3231.
13 C. C. Villa, N. M. Correa, J. J. Silber, F. Moyano and R. D. Falcone, *Phys. Chem. Chem. Phys.*, 2015, **17**, 17112–17121.
14 P. Ädelroth, *Biochim. Biophys. Acta*, 2006, **1757**, 867–870.
15 P. L. G. Chong and S. Capes. Wong, *Biochemistry*, 1989, **28**, 8358–8363.
16 J. Seelig, P. M. McDonald and P. G. Scherer, *Biochemistry*, 1987, **26**, 7535–7541.
17 P. H. Devaux and M. Signeuret, *Biochim. Biophys. Acta*, 1985, **822**, 63–125.
18 M. Ikonen, L. Murtomaki and K. Kontturi, *J. Electroanal. Chem.*, 2007, **602**, 189–194.
19 S. M. Ulmeanu, H. Jensen, G. Bouchard, P. A. Carrupt and H. H. Girault, *Pharm. Res.*, 2003, **20**, 1317–1322.
20 S. Kwakye, V. N. Goral and A. J. Baeumner, *Biosens. Bioelectron.*, 2006, **21**, 2217–2223.
21 S. Viswanathan, L. C. Wu, M. R. Huang and J. A. Ho, *Anal. Chem.*, 2006, **78**, 1115–1121.
22 J. A. P. Piedade, M. Mano, M. C. Pedroso de Lima, T. S. Oretskaya and A. M. Oliveira-Brett, *Biosens. Bioelectron.*, 2004, **20**, 975–984.
23 A. Sapper, B. Reiss, A. Janshoff and J. Wegener, *Langmuir*, 2006, **22**, 676–680.

24 J. A. Bard, X. Li and W. Zhan, *Biosens. Bioelectron.*, 2006, **22**, 461–472.
25 V. Agmo Hernandez and F. Scholz, *Langmuir*, 2006, **22**, 10723–10731.
26 D. Grieshaber, R. MacKenzie, J. Voros and E. Reimhult, *Sensors*, 2008, **8**, 1400–1458.
27 S. Niwa, M. Eswaramoorthy, J. Nair, A. Raj, N. Itoh, H. Shoji, T. Namba and F. Mizukami, *Science*, 2002, **295**, 105–107.
28 J. D. Meeker, L. Ryan, D. B. Barr, R. F. Herrick, D. H. Bennett, R. Bravo and R. Hauser, *Environ. Health Perspect.*, 2004, **112**, 1665–1670.
29 N. M. Correa, M. A. Biasutti and J. J. Silber, *J. Colloid Interface Sci.*, 1996, **184**, 570–578.
30 M. Novaira, M. A. Biasutti, J. J. Silber and N. M. Correa, *J. Phys. Chem. B*, 2007, **111**, 748–759.
31 R. D. Falcone, N. M. Correa and J. J. Silber, *Langmuir*, 2009, **25**, 10426–10429.
32 H. B. Bohidar and M. Behboudina, *Colloids Surf., A*, 2001, **178**, 313–323.
33 *CRC Handbook of Chemistry and Physics*, ed. M. Haynes, National institute of standards and technology, USA, 91st edn, 2010.
34 F. Moyano, J. J. Silber and N. M. Correa, *J. Colloid Interface Sci.*, 2008, **317**, 332–345.
35 N. M. Correa, D. H. Zorzan, M. Chiarini and G. Cerichelli, *J. Org. Chem.*, 2004, **69**, 8224–8230.
36 N. M. Correa, D. H. Zorzan, L. D'Anteo, E. Lasta, M. Chiarini and G. Cerichelli, *J. Org. Chem.*, 2004, **69**, 8231–8238.
37 S. S. Quintana, R. D. Falcone, J. J. Silber and N. M. Correa, *ChemPhysChem*, 2012, **13**, 115–123.
38 J. J. Silber, A. Biasutti, E. Abuin and E. Lissi, *Adv. Colloid Interface Sci.*, 1999, **82**, 189–252.
39 J. Sujatha and A. K. Mishra, *J. Photochem. Photobiol., A*, 1996, **101**, 215–219.
40 Y. V. Il'ichev, A. B. Demyashkevich and M. G. Kuzmin, *J. Phys. Chem.*, 1991, **95**, 3438–3444.
41 D. Mandal, S. K. Pal and K. Bhattacharyya, *J. Phys. Chem. A*, 1998, **102**, 9710–9714.
42 O. F. Silva, M. A. Fernández, J. J. Silber, R. H. Rossi and N. M. Correa, *ChemPhysChem*, 2012, **13**, 124–130.
43 N. M. Correa and J. J. Silber, *J. Mol. Liq.*, 1997, **72**, 163–176.
44 N. M. Correa, E. N. Durantini and J. J. Silber, *J. Colloid Interface Sci.*, 2001, **240**, 573–580.
45 R. D. Falcone, N. M. Correa, M. A. Biasutti and J. J. Silber, *J. Colloid Interface Sci.*, 2006, **296**, 356–364.